METEORITE WEATHERING ON MARS — UPDATES ON EXOGENIC IRON SURVIVABILITY BIASES AND MICRO-MAPPING OF MERIDIANI PLANUM BLOCK ISLAND MI MOSAICS.

J. W. Ashley[1] and K. E. Herkenhoff[2]; [1]Jet Propulsion Laboratory, California Institute of Technology, 4800 Oak Grove Drive, Pasadena, CA 91109-8099; [2]Astrogeology Science Center, U.S. Geological Survey, Flagstaff, AZ 86001. (james.w.ashley@jpl.nasa.gov).

Introduction: The *in-situ* and terrestrial analog study of martian finds (meteorites found on Mars) contributes to an array of science disciplines [e.g., 1-4]. Significantly for Mars science, these exogenic rocks provide opportunities to study a variety of martian Amazonian surface weathering processes. Their unique mineralogies, reactivities, freshness, and location (in near-equatorial martian environments) makes them ideal for studies of water occurrence and behavior, calibration of climate models, and associated astrobiological questions. The frequency of find occurrence at all three rover landing sites (Spirit, Opportunity, and Curiosity) validates anticipation of future finds for any planned roving spacecraft. Here we report updates on two aspects of meteorite weathering on Mars: 1) surface find inventory and population statistics as affected by chemical alteration; and 2) micro-mapping of oxide coatings on Microscopic Imager (MI) mosaics for the Block Island meteorite at Meridiani Planum.

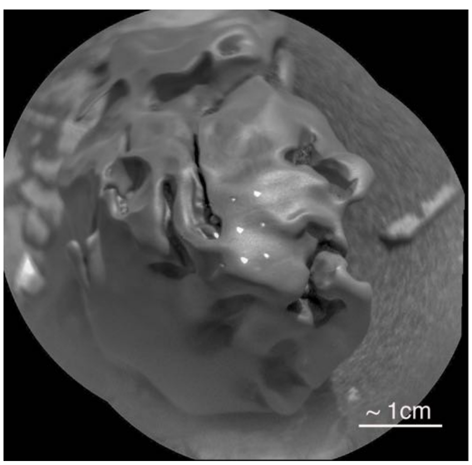

Figure 1. Egg Rock. Released raw image mosaic taken with ChemCam RMI. White spots near center are Laser-Induced Breakdown Spectrometer (LIBS) targets. Image credits: NASA/JPL-Caltech/LANL.

Meteorite Populations on Mars: With the October 30th, 2016 (sol 1505) find of the iron-nickel meteorite Egg Rock by the Curiosity rover on the Murray Formation (Figure 1), the inventory of confirmed and candidate meteorites identified on the martian surface has climbed to 22 finds. Publically released Mast Camera (MastCam) and Chemistry and Camera (ChemCam) Remote Micro-Imager (RMI) images are reviewed here for comparison with ongoing statistical and morphologic studies involving all other martian finds.

Egg Rock has a "gunmetal" surface color in color-corrected MastCam frames. A purple-hued patch is noted on the upper surface that appears to be outside the LIBS target area. Features resembling regmaglypts are debatable for the reasons outlined in [5]. No Widmanstätten patterns are evident within the area imaged. Deep incisions are found across the visible surface and do not appear consistent with an atmospheric ablation formation mechanism, but probably resulted from post-fall differential aeolian scouring. Unlike Block Island, Lebanon, and Littleton, no obvious signs of orientation are apparent among the surface scours.

Meteorite	Rover	First sol encountered	Type (suspected or confirmed)	Instrumentation employed
Heat Shield Rock*	Opportunity	339	IAB complex iron	MTES/Pancam/APXS/MB/MI
Block Island	Opportunity	1961	IAB complex iron	Pancam/APXS/MB/MI
Shelter Island	Opportunity	2022	IAB complex iron	Pancam/APXS/MB/MI
Mackinac Island	Opportunity	2034	iron	PancamNavcam
Oileán Ruaidh	Opportunity	2368	iron	PancamNavcam
Ireland	Opportunity	2374	iron	PancamNavcam
Bingag Cave	Opportunity	2642	iron	PancamNavcam
Dia Island	Opportunity	2642	iron	PancamNavcam
Allan Hills	Spirit	858	iron	MTES/Pancam/Navcam
Zhong Shan	Spirit	858	iron	MTES/Pancam/Navcam
Lebanon	Curiosity	634	iron	Mastcam/ChemCam RMI
Lebanon B	Curiosity	634	iron	Mastcam/ChemCam RMI
Littleton	Curiosity	634	iron	Mastcam/ChemCam RMI
Egg Rock	Curiosity	1505	iron	Mastcam/LIBS
Barberton	Opportunity	121	stony-iron	PancamNavcam
Santa Catarina	Opportunity	1034	stony-iron	MTES/Pancam/APXS/MB/MI
Joacaba	Opportunity	1046	stony-iron	MTES/Navcam
Mafra	Opportunity	1151	stony-iron	MTES/Navcam
Paloma	Opportunity	1190	stony-iron	MTES/Navcam
Santorini	Opportunity	1713	stony-iron	Pancam/APXS/MB/MI
Kasos	Opportunity	1889	stony-iron	Pancam/APXS/MB/MI
Canegrass	Opportunity	3346	stony	Pancam/Navcam

Figure 2. Inventory of meteorites found on Mars at three rover landing sites, color-organized by pairing assumptions.

With each new meteorite find, the ability to review and discuss population statistics and its relevance to Mars science improves. The question of pairing plays heavily here since it reduces the number of individual fall events. The 22 finds likely represent a significantly lower subset (six to nine) of individual fall events, depending on pairing assumptions. Pairing is based here on appearance (morphology, reflectance, color, etc.), and field occurrence (proximity) of the rocks. The "likelihood" for meteorite encounters during a given rover traverse is a qualitative impression based on cumulative driving experience for each landing site. Conservative pairing in Figure 2 assumes six iron and two non-iron (either stony or stony-iron) candidate falls for the planet.

[6] examined the preponderance of irons within this population, identifying what is almost certainly a sampling bias due to various mass/size-related factors. Research on the weathering behavior of Antarctic ordinary chondrites [e.g., 7], in concert with recently determined rates of weathering for stony meteorites in the martian setting [1], suggested that fragmentation due to one or more of 1) mass breakup during atmospheric flight, 2) impact, or 3) post-fall weathering, contributed to the small mass problem. Figure 3 presents pre-atmospheric populations of iron, stony, and

stony-iron meteorites (based on >1100 Earth falls [8]) with martian finds paired to represent a conservative number of fall events (eight). It is possible that all Meridiani irons represent a single fall event, but even then irons predominate well beyond the anticipated fraction, with chondritic meteorites anomalously low or absent.

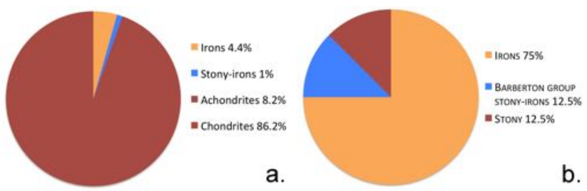

Figure 3. Meteorite fall percent fractions among iron (orange), stony (burgundy), and stony iron (blue) groups known for Earth (a) and paired for Mars (b) populations. Earth values group chondrites and achondrites within the stony category, and are based on >1100 witnessed falls. Mars finds are grouped according to assumptions outlined in text and Figure 2. The mode of identification of Egg Rock is consistent with a survivability bias for the predominance of irons on Mars, as opposed to a selection bias.

All meteorites found on Mars before Egg Rock were detected through panoramic remote sensing, which covers a much larger area and should therefore sample a more representative surface population. Thus, unless coincidental, the unplanned appearance of an iron meteorite within the Curiosity work volume lends support to a true iron-favoring, weathering-survival bias and not a science team-based selection bias. Otherwise a stony meteorite (94% of the pre-terrestrial population) would be expected for a serendipitous find, particularly one of Egg Rock's size. The rate of weathering during the Amazonian for stony meteorites, facilitated largely by metallic iron oxidation, has recently been estimated at roughly 10 times longer than meteorites in Antarctica [1]. The mechanism for fragmentation has been discussed in [5].

Block Island Microscopic Imager Mosaic Mapping: The effects of iron oxidation among stony meteorites is complimented in martian meteoritcs by its occurrence on iron meteorite surfaces, where it has partially survived and can be studied morphologically and chemically [4]. Here we report on the effort to prepare final micro-maps of Meridiani Planum Block Island meteorite surfaces using MI mosaics and ArcGIS mapping software. In addition to providing insights into responsible processes, mapping forces the consideration of contact relationships along full perimeters of each mappable "unit." Unit descriptions include one new mappable unit type (cS). Measurements of the morphology and spatial density of the Widmanstätten features are most consistent with schreibersite lamellae, not kamacite plates or taenite lamellae.

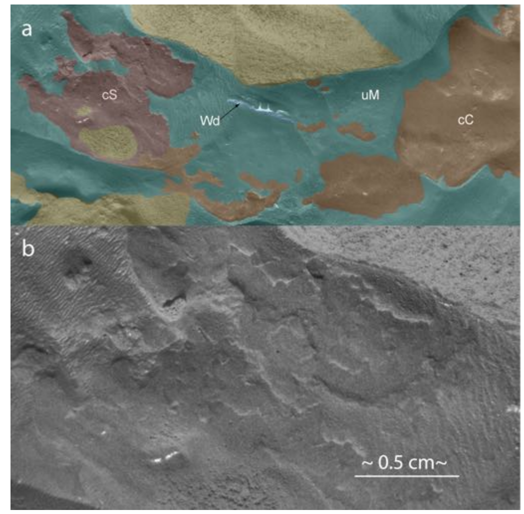

Figure 4. Sample of one of three Block Island MI mosaic maps, showing examples of stepped iron oxide coating (cS), together with previously recognized units (described below). Light yellow patches are accumulated dust.

Uncoated metal (uM) — moderate reflectance surface, often exhibiting pitted texture, which sometimes includes circular pit features, or sub-parallel grooves often showing braded or anastomosing patterns. Surfaces can appear sculpted, with sharp-edged peaks between hollows. Hollows themselves often show signs of enlargement and undercutting. *Interpretation*: Exposed metal surface, likely coated with thin dust layer (as demonstrated by Heat Shield Rock brush cleaning).

Conformable iron oxide coating (cC) — low reflectance surface, exhibiting topographic relief (evidenced by shadows) at some margins and thinning at other margins. Presents embayments, evidence of sculpting, and superposing relationships, *Interpretation*: Material has been identified by [9] to be iron oxide coating. Cross-cutting relationships establish post-fall formation timing. Softness and recent formation history evidenced by occurrence [5].

Stepped iron oxide coating (cS) — oxide coating with multiple tabular or layered appearance. *Interpretation*: The material represents either an example of multiple layering, presumably by surviving previous destructive cycles, or an exfoliating version of the conformable coating.

Widmanstätten pattern (Wd) — high- (often specular) reflectance features occurring in diagnostic octahedrite pattern with variable spacing and considerable surface relief. *Interpretation*: Differentially eroded schreibersite lamellae.

Acknowledgements: This research was funded in part by NASA grant NNN13D465T.

References: [1] Schröder C. *et al.*, (2016) *Nat Comm* 7, 13459. [2] Chappelow J. E. Golombek M. P. (2010) *J. Geophys. Res.* 113 E06S22. [3] Fleischer I. *et. al.,* (2011) *MAPS,* 46, issue 1, 21-34. [4] Ashley J. W. *et al.*, (2011) *JGR* 116, E00F09. [5] Ashley J. W. and Golombek M. P. (2016) *LPSC XLVII, abs.* # 2461. [6] Ashley J. W. (2014) *GSA* abs. #202-14. [7] Velbel M. A. (2014) *MAPS,* 49, issue 2, 154-171. [8] Meteoritical Bulletin Database. [9] Schröder C. et al., (2008) *J. Geophys. Res.* 113 E06S22.